UC Davis

UC Davis Previously Published Works

Title

Exogenous GLP-1 stimulates TCA cycle and suppresses gluconeogenesis and ketogenesis in late-fasted northern elephant seals pups

Permalink

https://escholarship.org/uc/item/8qm1t6rk

Journal

AJP Regulatory Integrative and Comparative Physiology, 320(4)

ISSN

0363-6119

Authors

Dhillon, Jaapna
Viscarra, Jose A
Newman, John W
et al.

Publication Date

2021-04-01

DOI

10.1152/ajpregu.00211.2020

Peer reviewed

eScholarship.org Powered by the California Digital Library
University of California

AMERICAN JOURNAL OF PHYSIOLOGY
REGULATORY, INTEGRATIVE AND COMPARATIVE PHYSIOLOGY

Am J Physiol Regul Integr Comp Physiol 320: R393–R403, 2021.
First published January 7, 2021; doi:10.1152/ajpregu.00211.2020

RESEARCH ARTICLE

Obesity, Diabetes and Energy Homeostasis

Exogenous GLP-1 stimulates TCA cycle and suppresses gluconeogenesis and ketogenesis in late-fasted northern elephant seals pups

Jaapna Dhillon,[1,2] Jose A. Viscarra,[1,3] John W. Newman,[4,5,7] Oliver Fiehn,[5] Daniel E. Crocker,[6] and Rudy M. Ortiz[1]

[1]*Department of Molecular & Cell Biology, School of Natural Sciences, University of California, Merced, California;* [2]*Department of Nutrition and Exercise Physiology, University of Missouri, Columbia, Missouri;* [3]*Department of Nutritional Sciences and Toxicology, University of California, Berkeley, California;* [4]*Obesity and Metabolism Research Unit, USDA Agricultural Research Service Western Human Nutrition Research Center, University of California, Davis, California;* [5]*NIH West Coast Metabolomics Center, University of California, Davis, California;* [6]*Department of Biology, Sonoma State University, Rohnert Park, California; and* [7]*Department of Nutrition, University of California, Davis, California*

Abstract

The postweaning fast of northern elephant seal pups is characterized by a lipid-dependent metabolism and associated with a decrease in plasma glucagon-like peptide-1 (GLP-1), insulin, and glucose and increased gluconeogenesis (GNG) and ketogenesis. We have also demonstrated that exogenous GLP-1 infusion increased plasma insulin despite simultaneous increases in cortisol and glucagon, which collectively present contradictory regulatory stimuli of GNG, ketogenesis, and glycolysis. To assess the effects of GLP-1 on metabolism using primary carbon metabolite profiles in late-fasted seal pups, we dose-dependently infused late-fasted seals with low (LDG; 10 pM/kg; n = 3) or high (HDG; 100 pM/kg; n = 4) GLP-1 immediately following a glucose bolus (0.5 g/kg), using glucose without GLP-1 as control (n = 5). Infusions were performed in similarly aged animals 6–8 wk into their postweaning fast. The plasma metabolome was measured from samples collected at five time points just prior to and during the infusions, and network maps constructed to robustly evaluate the effects of GLP-1 on primary carbon metabolism. HDG increased key tricarboxylic acid (TCA) cycle metabolites, and decreased phosphoenolpyruvate and acetoacetate ($P < 0.05$) suggesting that elevated levels of GLP-1 promote glycolysis and suppress GNG and ketogenesis, which collectively increase glucose clearance. These GLP-1-mediated effects on cellular metabolism help to explain why plasma GLP-1 concentrations decrease naturally in fasting pups as an evolved mechanism to help conserve glucose during the late-fasting period.

adipose; fatty acids; glucose intolerance; insulin resistance; insulin sensitivity

INTRODUCTION

Northern elephant seal pups (*Mirounga angustirostris*) undergo a 2- to 3-mo postweaning fast during which they remain normothermic and metabolically active, while relying primarily on the oxidation of stored lipids to meet their caloric needs (1–3). The natural, prolonged, postweaning fast of the northern elephant seal pup is associated with decreased insulin and increased glucagon and cortisol (4–7), which collectively would support a glucogenic endocrine profile. Furthermore, fasting is also associated with increased endogenous glucose production and ketogenesis to help support the growing demand for glucose with fasting (5, 8). Because fasting mammals depend primarily on lipids for energy, the decreased glucose uptake and utilization resulting from impaired insulin signaling preserves the limited carbohydrate substrates for tissues that do not readily metabolize lipids (e.g., central nervous system, red blood cells). In addition, as less glucose is used, less protein has to be broken down for gluconeogenesis (GNG), and thus lean tissue catabolism can be reduced (9). However, we have previously shown that high-dose, exogenous glucagon-like peptide-1 (GLP-1), an incretin hormone that facilitates postprandial insulin secretion (10), also induced increased cortisol and glucagon which collectively presents with contradictory regulatory stimuli of glucose. Regardless of the endocrine profile induced by exogenous GLP-1, the result was an increase in glucose clearance (utilization), which could be accomplished by appropriate changes in tricarboxylic acid (TCA) cycle activity, GNG, and ketogenesis among other mechanisms.

The postweaning fasts are also characterized by increased plasma free fatty acids, elevated plasma glucose, and

Correspondence: J. Dhillon (jdhillon@missouri.edu).
Submitted 16 July 2020 / Revised 16 December 2020 / Accepted 5 January 2021

0363-6119/21 Published by the American Physiological Society.

Downloaded from journals.physiology.org/journal/ajpregu by Rudy Ortiz (098.239.103.052) on April 7, 2021.

decreased cellular insulin signaling activity (2, 4, 11, 12), which collectively would constitute an insulin-resistance phenotype (13). Furthermore, we have previously reported significant reductions in the concentrations of insulin-sensitizing hormones adiponectin and IGF-1, along with significant increases in cortisol (14), which has been reported to antagonize insulin activity (15, 16). Prolonged fasting in pups is also characterized by decreased plasma insulin and reduced glucose-stimulated insulin secretion (GSIS) (14) suggesting that this period of absolute food deprivation is associated with impaired pancreatic responsiveness. The simultaneous fasting-induced reductions in GLP-1 and insulin are likely contributing to the insulin resistance observed in fasting seal pups to help preserve the relatively high-plasma glucose levels to support their energetic demands during this prolonged period of food deprivation. However, reductions in plasma levels do not necessarily imply a state of nonfunctionality. For example, despite the fasting-induced reductions in insulin, we have demonstrated that exogenous insulin infusion in late-fasted seal pups (when levels are the lowest) induced time-dependent changes in the phosphorylation of insulin receptor and downstream signaling proteins in adipose and muscle (although the cellular signaling events were suppressed compared with early-fasted pups in the same study) (7) and in the metabolome (17) suggesting that the tissues remain insulin sensitive. Given that GLP-1 facilitates GSIS and induces GLP-1 receptor-mediated cellular effects independent of insulin, we took a similar approach as with insulin and have shown that exogenous GLP-1 in late-fasted seal pups induced profound changes in their hormone profile and time-dependent changes in insulin receptor phosphorylation, again suggesting that tissues remain responsive to GLP-1 (7). However, the responsiveness and functionality of GLP-1 on cellular metabolism (as indicated by changes in the metabolome) in late-fasted seals was not examined previously. Therefore, to gain further insights on GLP-1-mediated effects on substrate metabolism and to better understand the paradoxical endocrine profile induced by high-dose GLP-1 on biochemical pathways, we employed complementary metabolomic approaches to more broadly examine the cellular effects of GLP-1 in late-fasted animals (when GLP-1 levels are the lowest).

Hence, the present study was designed to assess the cellular mechanisms contributing to the regulation of glucose during a lipid-based metabolism in prolonged food-deprived mammals. Because elephant seals have evolved robust physiological mechanisms that allow them to naturally tolerate protracted bouts of fasting, they provide an ideal model to examine the effects of fasting on insulin sensitivity and its associated pathways. To address the hypothesis that exogenous GLP-1 increases TCA cycle activity and suppresses GNG, we performed robust metabolomic analysis of primary carbon metabolites in late-fasted seal pups infused with an acute bolus of GLP-1.

METHODS

All procedures were reviewed and approved by the Institutional Animal Care and Use Committees of University of California, Merced and Sonoma State University. All work was realized under the National Marine Fisheries Service marine mammal permit no. 87-1743. Data presented here complements data from the same animals published previously (7, 14).

Animals

Northern elephant seal pups (n = 12) constituting three different cohorts at Año Nuevo State Reserve were studied during the late, postweaning period (6–8 wk postweaning) when animals experienced temporary and reversible insulin resistance characterized by: *1*) elevated plasma NEFA and cortisol and *2*) reduced plasma adiponectin, GLP-1, and insulin. Pups were weighed, sedated, and infused in the field as previously described (7, 11, 14).

GLP-1 Infusion Protocol

Before the infusion of GLP-1, a preinfused blood sample was collected from each animal as previously described (7, 14). GLP-1 was infused in a dose-dependent manner in the presence of glucose to allow for the differentiation between reduced insulin production and glucose intolerance. This experimental protocol was adopted because GLP-1 in the presence of elevated glucose has the potential to provide greater insight to GLP-1-mediated effects (7). Furthermore, the simultaneous infusion of glucose with GLP-1 helps to protect against the potential of inducing a consequential bout of hypoglycemia (18, 19). Twelve, late-fasted male seal pups were studied in the following groups: *1*) no GLP-1 + glucose (0.5 g/kg) [control; 92 (means) ± 6 (SD) kg; n = 5], *2*) low-dose GLP-1 (10 pmol/kg) + glucose (0.5 g/kg) (LDG; 98 ± 1 kg; n = 3), and *3*) high-dose GLP-1 (100 pmol/kg) + glucose (0.5 g/kg) (HDG; 94 ± 4 kg; n = 4). The GLP-1 (Sigma, St Louis, MO) was administered as a bolus immediately following a glucose bolus via an intravenous infusion within 2-min postglucose. Following the infusions, blood samples were collected at 10, 30, 60, and 120 min. Blood samples were centrifuged on-site for 15 min at 3,000 *g*, and the plasma was transferred to cryovials, frozen by immersion in liquid nitrogen, and stored at −80°C. GLP-1 + glucose manipulations were performed only on late-fasted animals because we and others have demonstrated that the insulin resistance-like conditions develop with fasting duration (5, 11, 12, 14, 20).

GCTOF Data Acquisition and Processing

The metabolite abundances in plasma samples were quantified by gas chromatography time-of-flight (GCTOF) mass spectrometry (MS) as previously described (21). Acquired mass spectra were processed using the BinBase database (22, 23). All entries in Bin-Base were matched against the Fiehn mass spectral library using retention index and mass spectrum information or the National Institute of Standards and Technology (NIST) 11 commercial library. Quality control procedures and data quality efforts have been described previously (17). Metabolites were reported if present in at least 50% of the samples.

Statistical Analyses

Data were reported as quantitative ion peak heights and were normalized by the sum intensity of all annotated

Downloaded from journals.physiology.org/journal/ajpregu by Rudy Ortiz (098.239.103.052) on April 7, 2021.

metabolites. The total area under the curve (AUC) over 120 min for each metabolite was calculated based on trapezoidal rule integration. Linear model analyses with *time 0* adjustment on the Johnson's transformed AUC values were conducted to determine the dose-dependent treatment effect. The false discovery rate (FDR) adjusted *P* values are also presented where treatment effect *P* values were adjusted for multiple hypotheses tested using Benjamini–Hochberg correction. Pairwise comparisons between treatment groups were conducted via *t* tests, and *P* values were adjusted for multiple testing using Tukey's honestly significant difference. All statistical analyses were performed using R version 3.6.2.

Network analysis was used to assess statistically significant results between control and HDG groups within a biochemical and structural context. A biochemical and chemical similarity network was created for all measured metabolites with KEGG and PubChem CID identifiers using MetaMapR (24). Metabolites involved in biochemical transformations were connected based on product-precursor relationships defined in the KEGG RPAIR database. Metabolites sharing structural properties defined in PubChem Substructure Fingerprints (25) were connected at a Tanimoto similarity threshold ≥ 0.7. The quantitative dataset composed of the fold changes, i.e., ratio of means (HDG/control) and treatment effect *P* values obtained from *time 0*-adjusted linear model tests (including only HDG and control groups). The network was then visualized in Cytoscape 3.7.2 (26) using the yFiles organic layout and visual separation of clusters in the network was facilitated with the GLay community clustering algorithm (27).

Chemical similarity enrichment analysis was conducted using ChemRICH, which is a software for metabolomics datasets that uses medical subject headings and Tanimoto substructure chemical similarity coefficients to cluster metabolites into nonoverlapping chemical groups (28). The quantitative dataset composed of the fold changes (ratio of means for HDG/control) and treatment effect (HDG vs. control) *P* values obtained from *time 0*-adjusted linear model tests (including only HDG and control groups). Statistically significant *P* values for clusters of metabolites were obtained by self-contained Kolmogorov–Smirnov tests and adjusted for FDR. For all analyses, it is important to note that changes in the time-course responses of metabolites are interpreted relative to other treatment groups and is not an indication of flux.

Table 1. *Total area under the curves over 120 min for selected metabolites measured following low- and high-dose GLP1 infusion in late-fasted northern elephant seal pups*

	Treatment			Treatment Effect		Pairwise Comparisons		
Metabolite	Control	LDG	HDG	*P* value (*time 0* adjusted)	FDR-adjusted, *P* value	LDG vs. Control	HDG vs. Control	LDG vs. HDG
2-Hydroxy-2-methylbutanoic acid	−0.55 ± 0.27	−0.18 ± 0.36	0.82 ± 0.3	0.026	0.169	0.720	**0.023**	0.151
2-Hydroxyvaleric acid	0.81 ± 0.19	−0.86 ± 0.26	−0.05 ± 0.22	0.002	0.076	**0.002**	**0.043**	0.100
2-Ketoisocaproic acid	0.94 ± 0.3	−0.88 ± 0.4	0.05 ± 0.34	0.019	0.168	**0.016**	0.183	0.243
3-Hydroxybutyric acid	0.77 ± 0.29	−0.46 ± 0.42	−0.62 ± 0.34	0.023	0.168	0.111	**0.029**	0.957
5-Methoxytryptamine	1.06 ± 0.34	−1.42 ± 0.34	−0.26 ± 0.33	0.005	0.132	**0.006**	0.113	**0.047**
Acetoacetate	0.7 ± 0.28	−0.57 ± 0.36	−0.57 ± 0.32	0.026	0.169	0.057	**0.041**	1.000
Aconitic acid	−1.28 ± 0.17	−0.99 ± 0.23	0.29 ± 0.19	0.001	0.061	0.583	**0.001**	**0.007**
Adenosine-5-monophosphate	0.9 ± 0.34	−0.89 ± 0.45	−0.46 ± 0.37	0.030	0.171	**0.040**	0.064	0.747
α-Aminoadipic acid	0.58 ± 0.35	−1.34 ± 0.44	0.28 ± 0.39	0.024	0.168	**0.024**	0.847	0.056
α-Ketoglutarate	−0.35 ± 0.21	−0.96 ± 0.25	0.58 ± 0.25	0.010	0.154	0.185	0.077	**0.008**
Aminomalonate	−0.9 ± 0.32	0.28 ± 0.43	0.91 ± 0.37	0.016	0.168	0.135	**0.015**	0.550
Aspartic acid	−0.41 ± 0.33	−0.25 ± 0.49	−2.09 ± 0.4	0.028	0.170	0.964	**0.028**	0.067
Benzoic acid	0.6 ± 0.25	−0.54 ± 0.31	−0.86 ± 0.28	0.011	0.154	**0.048**	**0.012**	0.732
Citric acid	−0.8 ± 0.26	0.15 ± 0.3	1.03 ± 0.3	0.009	0.154	0.091	**0.008**	0.161
Cystathionine	−1.5 ± 0.19	−2.04 ± 0.33	−0.54 ± 0.24	0.019	0.168	0.401	**0.030**	**0.029**
Cytosine	−0.04 ± 0.25	−0.23 ± 0.33	1.32 ± 0.29	0.012	0.154	0.890	**0.019**	**0.021**
Erythritol	−0.65 ± 0.22	−0.47 ± 0.39	0.84 ± 0.33	0.018	0.168	0.919	**0.015**	0.138
Glucose	−0.48 ± 0.29	0.01 ± 0.4	1.04 ± 0.33	0.024	0.168	0.612	**0.020**	0.194
Glutamine	1.08 ± 0.27	−1.62 ± 0.32	0.01 ± 0.26	0.001	0.076	**0.001**	0.073	**0.007**
Glyceric acid	−0.7 ± 0.32	1.04 ± 0.43	0.09 ± 0.39	0.031	0.172	**0.027**	0.337	0.332
Hexitol	−0.34 ± 0.18	0.56 ± 0.23	−0.23 ± 0.19	0.035	0.187	**0.036**	0.906	0.067
Isothreonic acid	−0.72 ± 0.21	−0.24 ± 0.31	0.81 ± 0.3	0.012	0.154	0.405	**0.011**	0.148
Lactamide	−0.9 ± 0.21	0.3 ± 0.27	0.73 ± 0.23	0.002	0.076	**0.019**	**0.002**	0.497
Lyxitol	−0.18 ± 0.29	−1.3 ± 0.44	1.05 ± 0.34	0.010	0.154	0.179	**0.049**	**0.011**
Malic acid	−0.37 ± 0.38	−0.64 ± 0.37	0.95 ± 0.4	0.037	0.187	0.886	0.166	**0.032**
Maltose	1.07 ± 0.42	−0.45 ± 0.46	−1.0 ± 0.45	0.048	0.232	0.114	**0.044**	0.661
N-ε-trimethyl-L-lysine	0.7 ± 0.35	−1.37 ± 0.44	0.16 ± 0.37	0.022	0.168	**0.020**	0.593	0.062
Octadecanol	−0.68 ± 0.32	0.91 ± 0.4	0.78 ± 0.33	0.028	0.170	**0.046**	**0.038**	0.960
Phosphoenolpyruvate	0.88 ± 0.3	−0.86 ± 0.42	−0.65 ± 0.33	0.013	0.154	**0.030**	**0.022**	0.926
Threitol	−0.45 ± 0.32	−0.6 ± 0.42	1.02 ± 0.38	0.037	0.187	0.961	**0.049**	0.058
Uric acid	−0.07 ± 0.2	−1.3 ± 0.25	1.06 ± 0.23	<0.001	0.061	**0.010**	**0.021**	**<0.001**
Xylose	−0.63 ± 0.29	−0.35 ± 0.42	0.99 ± 0.35	0.021	0.168	0.857	**0.018**	0.124

Treatment values are least square means ± SE (transformed values presented). FDR, false discovery rate; HDG, high-dose GLP-1 + glucose; LDG, low-dose GLP-1 + glucose. Metabolites were selected based on treatment effect *P* value < 0.05. Linear model analysis with *time 0* adjustment on transformed data. Pairwise comparisons were adjusted for multiple comparisons using Tukey's honestly significance difference. LDG, $n = 3$ seal pups; HDG; $n = 4$ seal pups; control, $n = 5$ seal pups. Values in bold indicate *P* value < 0.05.

Downloaded from journals.physiology.org/journal/ajpregu by Rudy Ortiz (098.239.103.052) on April 7, 2021.

RESULTS

Univariate Analyses Reveal Distinct Changes in Metabolites Induced by High-Dose GLP-1

A total of 398 metabolites were quantified by GCTOF MS of which 150 had known PubChem identifiers. The AUC over 120 min for 32 known metabolites (i.e., 21%) showing significant ($P < 0.05$) overall treatment effects are shown in Table 1 and the time-response curves for the infusions are depicted in Fig. 1-3. It should be noted that the values and effects presented in Table 1 have been adjusted for *time 0*. The time-response curves are of the unadjusted data (Fig. 1, 2, and 3, *A–H*). As an example of what *time 0*-adjusted curves look like, the intensities of xylose relative to *time 0* have been plotted in Fig. 3. The metabolic pathway designations of these metabolites are shown in Table 2. In this dose-dependent analysis, HDG elicited greater AUCs than LDG only ($P < 0.05$) for malic acid and α-ketoglutarate, and no significant differences were detected between HDG and control, and LDG and control. For

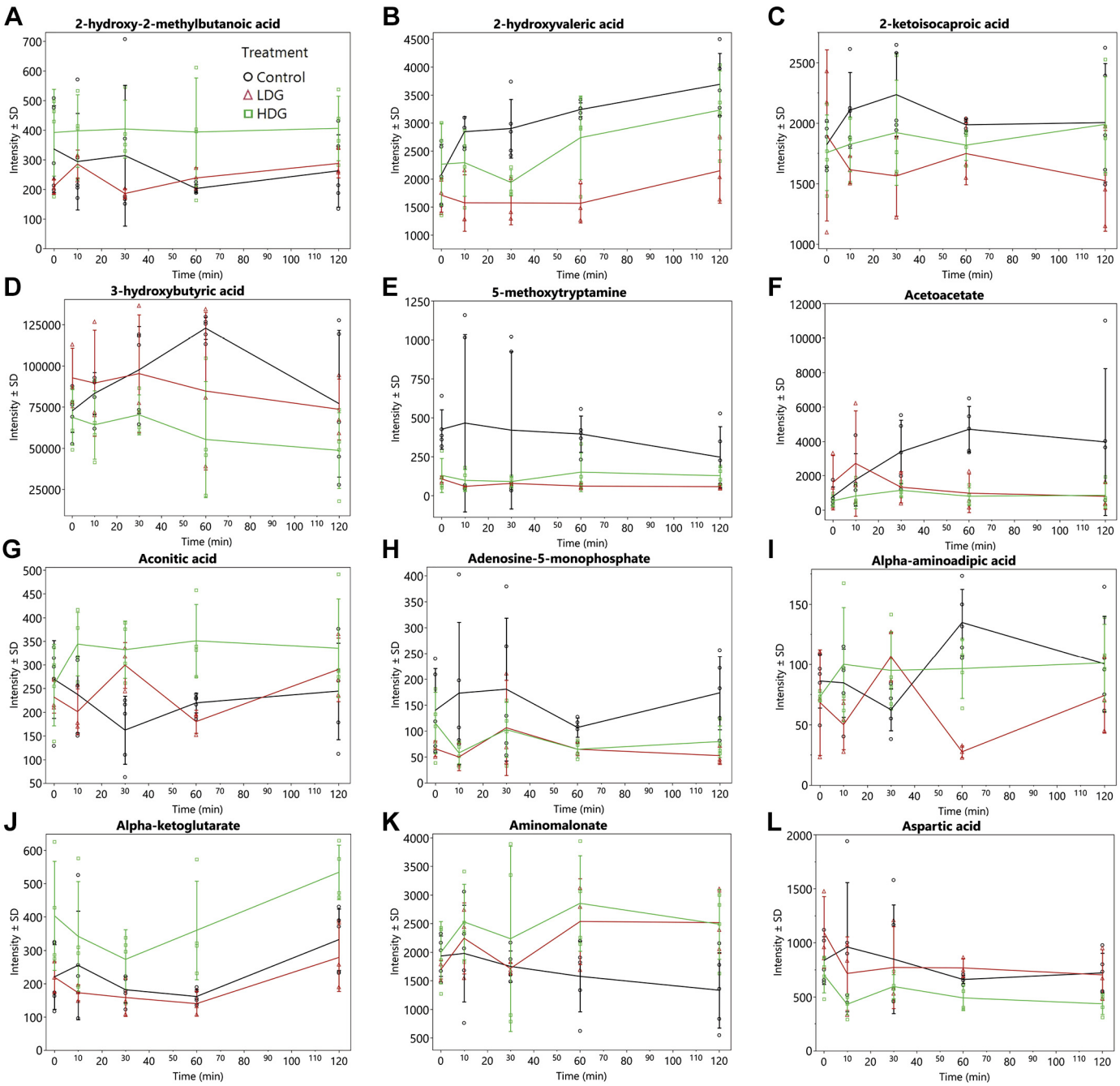

Figure 1. Mean intensities ± SD of metabolic trajectories (over 120 min) for 2-hydroxy-2-methylbutanoic acid (*A*), 2-hydroxyvaleric acid (*B*), 2-ketoisocaproic acid (*C*), 3-hydroxybutyric acid (*D*), 5-methoxytryptamine (*E*), acetoacetate (*F*), aconitic acid (*G*), adenosine-5-monophosphate (*H*), α-aminoadipic acid (*I*), α-ketoglutarate (*J*), aminomalonate (*K*), and aspartic acid (*L*). These metabolites indicated significant (*P* value < 0.05) overall treatment effects for AUCs (Table 1) in late-fasted elephant seals. LDG, $n = 3$ seal pups; HDG; $n = 4$ seal pups; control, $n = 5$ seal pups. Values are unadjusted and nontransformed.

Downloaded from journals.physiology.org/journal/ajpregu by Rudy Ortiz (098.239.103.052) on April 7, 2021.

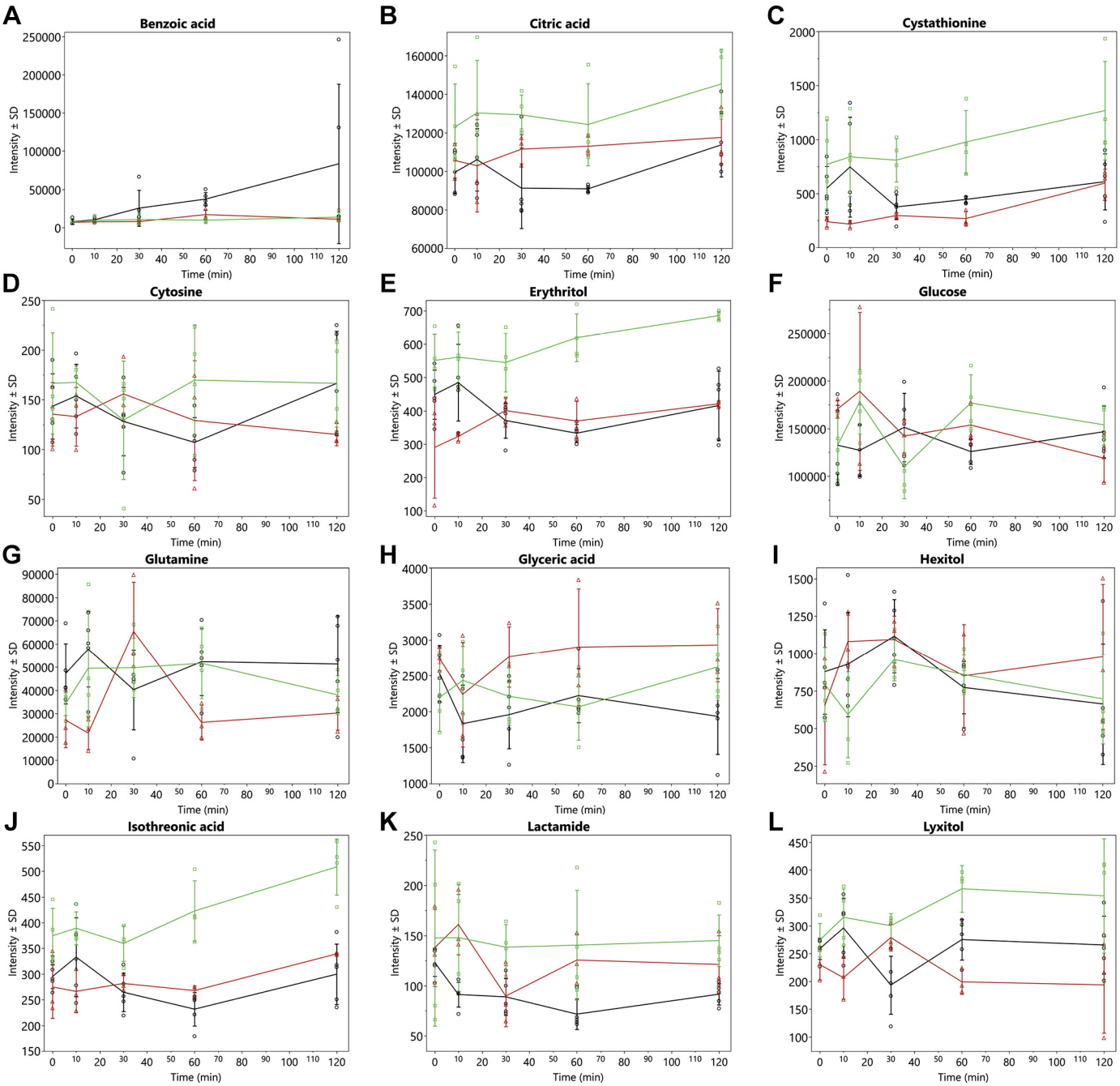

Figure 2. Mean intensities ± SD of metabolic trajectories (over 120 min) for benzoic acid (*A*), citric acid (*B*), cystathionine (*C*), cytosine (*D*), erythritol (*E*), glucose (*F*), glutamine (*G*), glyceric acid (*H*), hexitol (*I*), isothreonic acid (*J*), lactamide (*K*), and lyxitol (*L*). These metabolites indicated significant (P value $<$ 0.05) overall treatment effects for AUCs (Table 1) in late-fasted elephant seals. LDG (red), n = 3 seal pups; HDG (green); n = 4 seal pups; control (black), n = 5 seal pups. Values are unadjusted and nontransformed.

aconitic acid, cystathionine, cytosine, and lyxitol, HDG elicited greater AUCs than LDG and control groups ($P <$ 0.05). For glutamine and 5-methoxytryptamine, HDG elicited greater AUCs than LDG, but LDG suppressed their AUCs compared with control ($P < 0.05$). For 2-hydroxy-2-methylbutanoic acid, aminomalonate, citric acid, erythritol, glucose, isothreonic acid, threitol, and xylose, HDG elicited greater AUCs than control group only ($P < 0.05$) (Table 1). For 3-hydroxybutyric acid, acetoacetate, aspartic acid, and maltose, HDG suppressed AUC compared with control group ($P < 0.05$), but no significant difference between LDG and control groups was detected (Table 1).

For uric acid, HDG infusions elicited greater AUCs than LDG and control, but control elicited greater AUCs than LDG infusions ($P < 0.05$, Table 1). For other metabolites such as lactamide and octadecanol, both HDG and LDG infusions resulted in greater AUCs than control, and for 2-hydroxyvaleric acid, benzoic acid, and phosphoenolpyruvate, both HDG and LDG infusions suppressed AUCs relative to control ($P <$ 0.05, Table 1). For glyceric acid and hexitol, LDG elicited

Downloaded from journals.physiology.org/journal/ajpregu by Rudy Ortiz (098.239.103.052) on April 7, 2021.

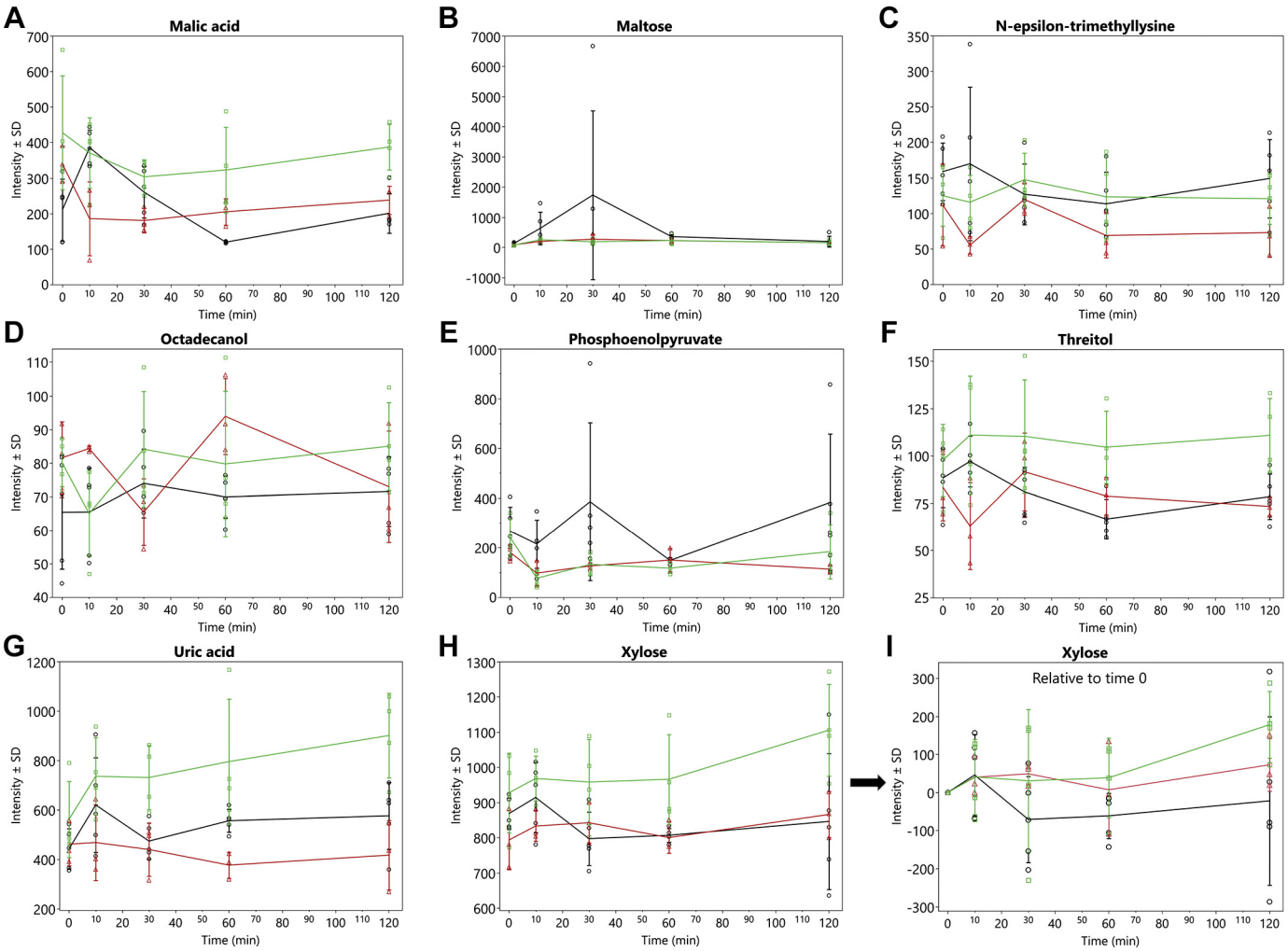

Figure 3. Mean intensities ± SD of metabolic trajectories (over 120 min) for malic acid (*A*), maltose (*B*), *N*-ε-trimethyllysine (*C*), octadecanol (*D*), phosphoenolpyruvate (*E*), threitol (*F*), uric acid (*G*), and xylose (*H*). These metabolites indicated significant (P value < 0.05) overall treatment effects for AUCs (Table 1) in late-fasted elephant seals. LDG, $n = 3$ seal pups; HDG; $n = 4$ seal pups; control, $n = 5$ seal pups. Values are unadjusted and nontransformed. *I*: metabolic trajectory of xylose relative to *time 0*.

greater AUCs than control, and for adenosine-5-monophosphate, 2-ketoisocaproic acid, α-aminoadipic acid, and *n*-epsilon-trimethyllysine, LDG suppressed AUCs relative to control ($P < 0.05$, Table 1).

The lack of consistent dose-dependent differences between control, LDG, and HDG groups suggests that these metabolic pathways are insensitive to low-dose GLP-1 in late-fasted conditions. Because the treatment effect analyses revealed distinct differences between the control and HDG groups for most metabolites (Table 1), only the fold changes of the AUCs of HDG group (vs. control) were included in the network and chemical similarity analyses.

Network Analysis of Metabolite AUCs Largely Depicts an Alteration in Compounds Involved in Amino Acid and Carbohydrate Metabolism in Response to High-Dose GLP-1 Infusion

The 121 identified metabolites with known PubChem and KEGG identifiers were clustered into groups based on biochemical and structural similarity. Four network clusters were largely based on structural similarity: amino acids and amines, carbohydrates, fatty alcohols, and lipids (Fig. 4). Two network clusters comprised predominantly of intermediate metabolites involved in the TCA cycle, and metabolites involved in nucleotide and energy metabolism, respectively (Fig. 4).

Amino acid metabolism.

Several metabolites involved in amino acid metabolism such as benzoic acid, creatinine, aspartic acid, glutamic acid, and glutamine were lower (0.25- to 0.94-fold change) and aminomalonate and cystathionine were higher (1.6- to 1.9-fold change) in response to HDG infusion relative to control ($P < 0.05$, Fig. 4).

Carbohydrate metabolism.

HDG infusion elicited a 1.1- to 1.7-fold change in metabolites largely involved in carbohydrate metabolism such as glucose, myo-inositol, xylose, lyxitol, citric acid, xylitol, aconitic acid, 2-hydroxyglutaric acid, malic acid, and α-ketoglutarate,

Downloaded from journals.physiology.org/journal/ajpregu by Rudy Ortiz (098.239.103.052) on April 7, 2021.

Table 2. *KEGG Pathway identifiers of selected metabolites measured following low- and high-dose GLP1 infusion in late-fasted northern elephant seal pups*

Metabolite	Metabolite Type	Metabolite Pathway
2-Hydroxyglutaric acid	Glutarates	Butanoate metabolism; C5-Branched dibasic acid metabolism
2-Hydroxy-2-methylbutanoic acid	Butyrates	Lipid metabolism[a]
2-Ketoisocaproic acid	Keto acids	Valine, leucine and isoleucine degradation; Valine, leucine and isoleucine biosynthesis; Glucosinolate biosynthesis
Acetoacetate	Keto acid	Synthesis and degradation of ketone bodies; Valine, leucine and isoleucine degradation; Lysine degradation; Tyrosine metabolism; Propanoate metabolism; Butanoate metabolism
Aconitic acid	Tricarboxylic acid	Citrate cycle (TCA cycle); Glyoxylate and dicarboxylate metabolism; C5-Branched dibasic acid metabolism
Adenosine-5-monophosphate	Adenine nucleotide	Purine metabolism
α-Aminoadipic acid	Dicarboxylic acids	Lysine biosynthesis; Lysine degradation
α-Ketoglutarate	Glutarate	Citrate cycle (TCA cycle); Pentose and glucuronate interconversions; Ascorbate and aldarate metabolism; Arginine biosynthesis; Alanine, aspartate and glutamate metabolism; Lysine biosynthesis; Lysine degradation; Histidine metabolism; Taurine and hypotaurine metabolism; D-Glutamine and D-glutamate metabolism; Glyoxylate and dicarboxylate metabolism; Butanoate metabolism; C5-Branched dibasic acid metabolism
Aminomalonate	Dicarboxylic acid	Amino acid metabolism
Aspartic acid	Amino acid	Amino acid metabolism
Benzoic acid	Carbocyclic acid	Phenylalanine metabolism; Benzoate degradation; Dioxin degradation; Toluene degradation; Aminobenzoate degradation
Cholesterol	Cholestenes	Steroid biosynthesis; Primary bile acid biosynthesis; Steroid hormone biosynthesis; Steroid degradation; Biosynthesis of alkaloids derived from terpenoid and polyketide
Citric acid	Tricarboxylic acid	Citrate cycle (TCA cycle); Alanine, aspartate and glutamate metabolism; Glyoxylate and dicarboxylate metabolism
Creatinine	Imidazole	Arginine and proline metabolism
Cystathionine	Amino acid	Amino acid metabolism
Cytosine	Pyrimidinones	Pyrimidine metabolism
Erythritol	Sugar alcohol	Sugar alcohol metabolism[a]
Glucose	Hexose	Glycolysis/Gluconeogenesis; Pentose phosphate pathway
Glutamic acid	Amino acid	Arginine biosynthesis; Alanine, aspartate and glutamate metabolism; Arginine and proline metabolism; Histidine metabolism; Taurine and hypotaurine metabolism; D-Glutamine and D-glutamate metabolism; Glutathione metabolism; Neomycin, kanamycin and gentamicin biosynthesis; Glyoxylate and dicarboxylate metabolism; Butanoate metabolism; C5-Branched dibasic acid metabolism; Nitrogen metabolism
Glutamine	Amino acid	Arginine biosynthesis; Purine metabolism; Pyrimidine metabolism; Alanine, aspartate and glutamate metabolism; D-Glutamine and D-glutamate metabolism; Glyoxylate and dicarboxylate metabolism; Vitamin B6 metabolism; Nitrogen metabolism; Aminoacyl-tRNA biosynthesis
Glyceric acid	Sugar acids	Pentose phosphate pathway; Glycine, serine and threonine metabolism; Glycerolipid metabolism; Glyoxylate and dicarboxylate metabolism; Methane metabolism
Hexitol	Sugar alcohols	Fructose and mannose metabolism
Hydroxybutyric acid	Hydroxybutyrate	Synthesis and degradation of ketone bodies; Butanoate metabolism
Isocitric acid	Tricarboxylic acid	Citrate cycle (TCA cycle)
Isoleucine	Amino acid	Amino acid metabolism
Isothreonic acid	Butyrate	Ascorbate and aldarate metabolism[a]
Lactamide	Amide	Cryoprotectant[a]
Lyxitol	Sugar alcohol	Sugar alcohol metabolism[a]; Pentose and glucuronate interconversions
Malic acid	Dicarboxylic acid	Citrate cycle (TCA cycle); Pyruvate metabolism; Glyoxylate and dicarboxylate metabolism; Methane metabolism
Maltose	Disaccharides	Starch and sucrose metabolism
Myo-inositol	Sugar alcohol	Galactose metabolism; Ascorbate and aldarate metabolism; Inositol phosphate metabolism
N-ε-trimethy-L-lysine	Amines	Carnitine synthesis[a]
Nicotinic acid	Nicotinic acids	Nicotinate and nicotinamide metabolism; Tropane, piperidine and pyridine alkaloid biosynthesis; Biosynthesis of plant secondary metabolites; Biosynthesis of alkaloids derived from ornithine, lysine and nicotinic acid
Octadecanol	Fatty alcohol	Lipid metabolism[a]
Phenylacetic acid	Carbocyclic acid	Phenylalanine metabolism
Phosphoenolpyruvate	Hydroxy acid	Glycolysis/Gluconeogenesis; Citrate cycle (TCA cycle); Phenylalanine, tyrosine and tryptophan biosynthesis; Phosphonate and phosphinate metabolism; Pyruvate metabolism; Methane metabolism

Continued

Downloaded from journals.physiology.org/journal/ajpregu by Rudy Ortiz (098.239.103.052) on April 7, 2021.

Table 2.— *Continued*

Metabolite	Metabolite Type	Metabolite Pathway
Succinic acid	Dicarboxylic acid	Citrate cycle (TCA cycle); Oxidative phosphorylation; Alanine, aspartate and glutamate metabolism; Lysine degradation; Tyrosine metabolism; Phenylalanine metabolism; Pyruvate metabolism; Glyoxylate and dicarboxylate metabolism; Propanoate metabolism; Butanoate metabolism
Threitol	Sugar alcohol	Sugar alcohol metabolism[a]
Tyrosine	Amino acid	Ubiquinone and other terpenoid-quinone biosynthesis; Tyrosine metabolism; Phenylalanine metabolism; Phenylalanine, tyrosine and tryptophan biosynthesis; Cyanoamino acid metabolism; Methane metabolism; Thiamine metabolism
Uric acid	Xanthine	Purine metabolism
Xylitol	Sugar alcohol	Sugar alcohol metabolism[a]; Pentose and glucuronate interconversions
Xylose	Monosaccharide	Carbohydrate metabolism

TCA, tricarboxylic acid. [a]Obtained from literature, not KEGG pathway identifiers.

0.51-fold change in phosphoenolpyruvate, and 0.32-fold change in maltose relative to control ($P < 0.05$, Fig. 4).

Lipid metabolism.

HDG infusion also elicited a 0.86-fold change in cholesterol, 0.24-fold change in acetoacetate, and 0.59-fold change in 3-hydroxybutyric acid relative to control ($P < 0.05$, Fig. 4). The free fatty alcohol, 1-octadecanol, was higher (1.1-fold) in response to HDG infusion relative to control ($P < 0.05$, Fig. 4).

Nucleotide metabolism.

HDG infusion elicited a 1.4-fold change in uric acid, 1.2-fold change in cytosine, and a 0.52-fold change in adenosine-5-monophosphate relative to control ($P < 0.05$, Fig. 4).

Other.

The sugar alcohols, erythritol and threitol were higher (1.5- and 1.4-fold, respectively), and the compound nicotinic acid which is involved in metabolism of cofactors and vitamins

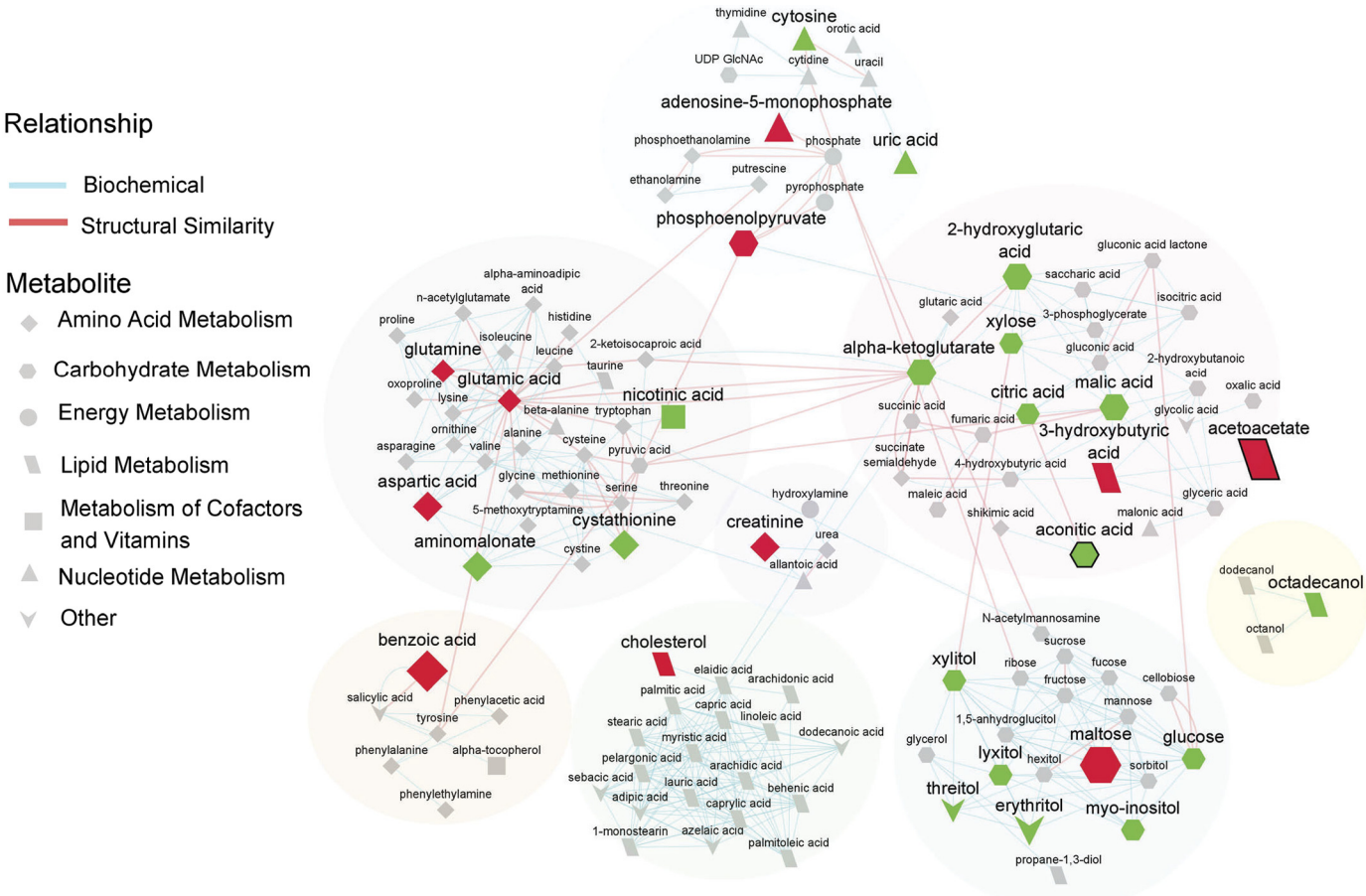

Figure 4. Biochemical network displaying differences between high-dose GLP-1 + glucose (HDG) and control groups. Metabolites are connected based on biochemical relationships (orange, KEGG RPAIRS) or structural similarity (blue, Tanimoto coefficient ≥ 0.7). Metabolite size denotes fold change of area under the curves (AUCs) between HDG and control). Metabolite color represents the relative change [green, higher ($P < 0.05$); red, lower ($P < 0.05$); gray, no difference (P value ≥ 0.05)] in response to HDG vs. control. P values obtained from *time 0* adjusted linear model analysis. Shapes display primary metabolic pathways and those metabolites with false discovery rate (FDR)-adjusted P value < 0.1 are highlighted with thick black borders. Clusters of metabolites are circled. HDG, $n = 4$ seal pups; control, $n = 5$ seal pups.

Downloaded from journals.physiology.org/journal/ajpregu by Rudy Ortiz (098.239.103.052) on April 7, 2021.

was also higher (1.2-fold) in response to HDG infusion relative to control ($P < 0.05$, Fig. 4).

Chemical Similarity Enrichment Analysis of Metabolites Indicates an Increase in Sugar Alcohol and Tricarboxylic Acids Clusters in Response to High-Dose GLP-1 Infusion

ChemRICH mapped 149 of the identified metabolites to 22 nonoverlapping chemical classes, of which 2 were significantly different between the control and HDG groups (FDR adjusted P value < 0.1). HDG was associated with higher clusters of sugar alcohols and tricarboxylic acids compared with control (Table 3). The key metabolites in these clusters were erythritol (sugar alcohol cluster) with a 1.5-fold change and aconitic acid (tricarboxylic acids cluster) with a 1.6-fold change in response to HDG infusion (vs. control). HDG was also associated with a higher cluster of glutarates and lower cluster of hydroxybutryates ($P < 0.05$ but FDR > 0.1, Table 3).

DISCUSSION

The protracted fasting of the northern elephant seal is a remarkable physiological feat that is well coordinated by exquisite regulation of cellular metabolism. We have shown that the ability to tolerate prolonged fasting periods is accomplished in part by temporary adipose-specific insulin resistance (7) and the maintenance of a lipid-based metabolism (based on static RQ = 0.71–0.73 (3, 29, 30)). Although lipid may serve as the primary source of energy for prolong-fasted seals, this does not preclude the potential for dynamic shifts in other metabolic processes that may results in changes in other classes of metabolites such as sugar alcohols and TCA cycle intermediates. Furthermore, we have also demonstrated that a high dose of the incretin, GLP-1, increased the clearance of glucose in late-fasted seals suggesting that GLP-1 facilitates glucose utilization (7). The present study provides complementary insights on the shifts in cellular metabolism induced by GLP-1 using a multi dose approach. We show here that high-dose GLP-1 induces higher time-course responses to *1*) TCA cycle metabolites and sugar alcohols, *2*) glucose metabolism, and *3*) lower responses to amino acid catabolism and ketogenesis (Fig. 5) relative to control.

GLP-1 Stimulates TCA Cycle and Suppresses Gluconeogenesis Relative to Control

Fasting duration in elephant seal pups is associated with the suppression of plasma GLP-1 (7) and insulin (7, 31), and an increase in circulating cortisol (6, 7, 31). However, we have previously shown that a high dose of GLP-1 increased the clearance (utilization) of glucose associated with increased plasma insulin despite increased cortisol and glucagon suggesting that the combined effects of high-dose GLP-1 on the proglycolytic mechanisms were substantially greater than the proglucogenic mechanisms (7). In the present study, the greater time-course responses of key TCA cycle metabolites to GLP-1 suggest that TCA cycle activity was increased resulting in increased glycolysis, contributing to the high-dose GLP-1-associated increase in glucose clearance observed previously (7). Furthermore, the lowered time-course response of phosphoenolpyruvate in the present study suggests that high-dose GLP-1 promotes glycolysis and suppresses GNG. Interestingly, high-dose GLP-1 promoted the generation of sugar alcohols, which are final metabolites of glucose metabolism. The greater time-course response of sugar alcohols substantiates the previously observed increase in glucose clearance/utilization associated with high-dose GLP-1 (7). Although sugar alcohols are used as low-calorie, dietary sweeteners (especially erythritol), which are not metabolized systemically in vivo, the greater levels of sugar alcohols here likely provides little if any metabolic benefit (32). However, the higher levels here are indicative of increased glucose metabolism (oxidation).

GLP-1 Suppresses Amino Acid Catabolism and Ketogenesis Relative to Control

The majority of metabolites involved in amino acid metabolism that demonstrated changes in response to high-dose GLP-1 were lowered relative to control with two

Table 3. *Chemical similarity enrichment analysis results of significant clusters of metabolites measured following high-dose GLP1 infusion (compared to control) in late-fasted northern elephant seal pups*

Cluster Name	Cluster Size	*P* Value (KS)	FDR Adjusted *P* Value (KS)	No. of Altered Metabolites in Cluster	Metabolites	*P*-Value Adjusted for *Time 0* (HDG vs. Control)	Fold Change of Means (HDG/ Control)
Sugar alcohols	9	0.0006	0.0066	Higher: 5, No change: 4	Erythritol	0.016	1.5
					Lyxitol	0.032	1.3
					Myo-inositol	0.016	1.1
					Threitol	0.016	1.4
					Xylitol	0.032	1.5
Tricarboxylic acids	3	0.00017	0.0038	Higher: 2, No change: 1	Aconitic acid	0.0011	1.6
					Citric acid	0.0075	1.3
Glutarates	3	0.016	0.12	Higher: 2, No change: 1	2-Hydroxyglutaric acid	0.017	1.6
					α-Ketoglutarate	0.021	1.7
Hydroxybutyrates	5	0.045	0.24	Lower: 2, No change: 3	3-Hydroxybutyric acid	0.0075	0.59
					2-Hydroxyvaleric acid	0.03	0.82

HDG, high-dose GLP-1 + glucose; KS, Kolmogorov–Smirnov test. HDG, n = 4 seal pups; control, n = 5 seal pups.

Downloaded from journals.physiology.org/journal/ajpregu by Rudy Ortiz (098.239.103.052) on April 7, 2021.

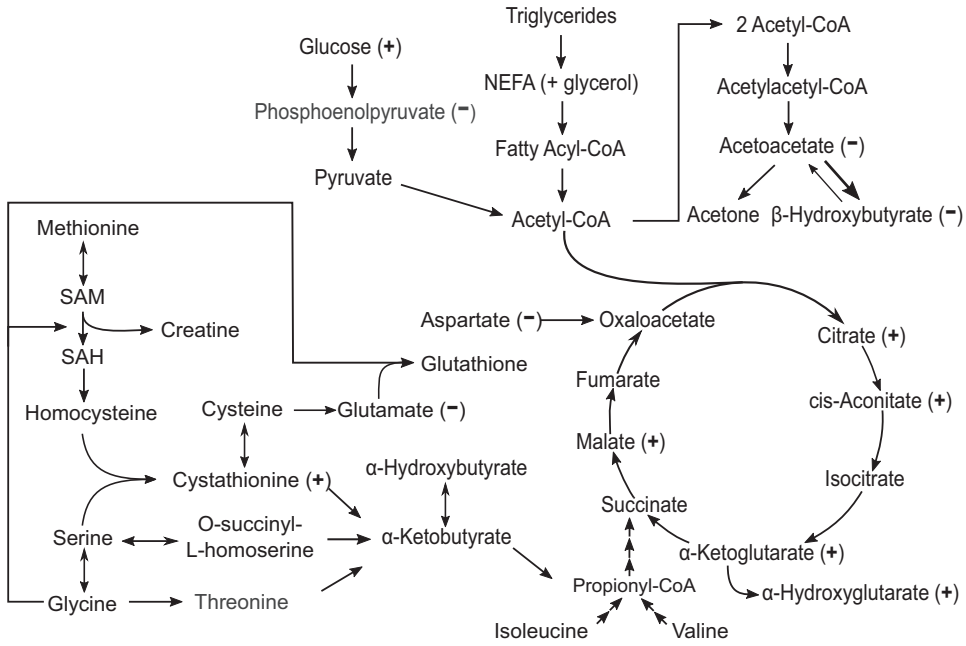

Figure 5. Schematic of metabolic pathways influenced by HDG infusions. *Time 0* adjusted linear model analysis. (+), significantly (P value < 0.05) higher in response to HDG vs. control; (−), significantly (P value < 0.05) lower in response to HDG vs. control. HDG, High dose GLP-1 + glucose. HDG; $n = 4$ seal pups; control, $n = 5$ seal pups.

exc-eptions suggesting that overall, protein catabolism was reduced. The effects of GLP-1 on suppressing protein metabolism, while they may be physiologically relevant, are likely minimal as protein catabolism is already relatively low, contributing to no more than 4% of energetic demands in fasting seal pups (1, 29). The lower time-course responses of 3-hydroxybutyric acid and acetoacetate to high-dose GLP-1 infusions suggest that ketogenesis is suppressed in response to high-dose GLP-1. During natural fasting conditions in elephant seal pups, β-hydroxybutyrate increases within the first 8 wk of the fast (8, 33). Under normal conditions, glucagon stimulates whereas insulin inhibits ketogenesis. We have previously shown that GLP-1 simultaneously induces an increase in glucagon and insulin in fasting elephant seal pups (7), presenting a contradictory regulatory stimuli of ketogenesis. Despite this contradictory evidence, the metabolomics data suggests that ketogenesis is suppressed suggesting that in fasting seal pups, insulin out-competes glucagon for the regulation of ketogenesis. This is further substantiated by previous studies that demonstrate that: *1*) insulin infusion in fasting seal pups suppresses β-hydroxybutyric acid (17) and *2*) the natural increase in ketones (8) is associated with reduced insulin (31, 33).

Perspectives and Significance

Collectively, these changes help substantiate the biochemical relevance of the natural reductions in GLP-1 and insulin with fasting duration. Fasting is characterized by: *1*) relatively high endogenous glucose production (5), *2*) increased ketogenesis through the first 8 wk of fasting, and *3*) sustained reduction in protein catabolism (1, 29, 33). Our data in late-fasted animals suggest that GLP-1 promotes glycolysis, and suppresses GNG, ketogenesis, and protein catabolism. Thus, the natural reduction in GLP-1 with fasting duration is likely an adaptive response to allow for the maintenance of relatively high-endogenous glucose production and suppressed glycolysis and protein catabolism as biochemical mechanisms to conserve circulating glucose and lean tissue.

ACKNOWLEDGMENTS

We thank Año Nuevo State Reserve for logistic support of this work and Drs. M. Thorwald, B. Martinez, and J. G. Sonanez-Organis for assistance in the field.

GRANTS

This study was supported by National Heart, Lung, and Blood Institute (NHLBI) Grant HL091767 (to R. M. Ortiz), NHLBI Grant HL091767-S1 (to R. M. Ortiz), and NHLBI Grant K02HL103787 (to R. M. Ortiz), and National Institute of Diabetes and Digestive and Kidney Diseases (NIDDK) Grant DK097154 (to O. Fiehn). Additional support was provided by USDA Intramural project Grant 2032-51530-022-00D and 2032-51530-025-00D (to J. W. Newman). The USDA is an equal opportunity provider, and employer.

DISCLOSURES

No conflicts of interest, financial or otherwise, are declared by the authors.

AUTHOR CONTRIBUTIONS

J.A.V. and R.M.O. conceived and designed research; J.A.V., D.E.C., and R.M.O. performed experiments; J.D. analyzed data; J.D., J.W.N., O.F., and R.M.O. interpreted results of experiments; J.D. and J.W.N. prepared figures; J.D. and R.M.O. drafted manuscript; J.D., J.W.N., O.F., D.E.C., and R.M.O. edited and revised manuscript; J.D., J.A.V., J.W.N., O.F., D.E.C., and R.M.O. approved final version of manuscript.

Downloaded from journals.physiology.org/journal/ajpregu by Rudy Ortiz (098.239.103.052) on April 7, 2021.

ENDNOTE

At the request of the authors, readers are herein alerted to the fact that additional materials related to this manuscript may be found at the institutional Web site of the authors, which at the time of publication they indicate is http://dx.doi.org/10.21228/M84S36. These materials are not a part of this manuscript and have not undergone peer review by the American Physiological Society (APS). APS and the journal editors take no responsibility for these materials, for the Web site address, or for any links to or from it.

REFERENCES

1. **Adams SH**, **Costa DP.** Water conservation and protein metabolism in northern elephant seal pups during the postweaning fast. *J Comp Physiol B* 163: 367–373, 1993. doi:10.1007/BF00265640.
2. **Castellini MA**, **Costa DP**, **Huntley AC.** Fatty acid metabolism in fasting elephant seal pups. *J Comp Physiol B* 157: 445–449, 1987. doi:10.1007/BF00691828.
3. **Ortiz CL**, **Costa D**, **Le Boeuf BJ.** Water and energy flux in elephant seal pups fasting under natural conditions. *Physiol Zool* 51: 166–178, 1978. doi:10.1086/physzool.51.2.30157864.
4. **Champagne CD**, **Houser DS**, **Crocker DE.** Glucose production and substrate cycle activity in a fasting adapted animal, the northern elephant seal. *J Exp Biol* 208: 859–868, 2005. doi:10.1242/jeb.01476.
5. **Houser DS**, **Champagne CD**, **Crocker DE.** Lipolysis and glycerol gluconeogenesis in simultaneously fasting and lactating northern elephant seals. *Am J Physiol Regul Integr Comp Physiol* 293: R2376–R2381, 2007. doi:10.1152/ajpregu.00403.2007.
6. **Ortiz RM**, **Wade CE**, **Ortiz CL.** Effects of prolonged fasting on plasma cortisol and TH in postweaned northern elephant seal pups. *Am J Physiol Regul Integr Comp Physiol* 280: R790–R795, 2001. doi:10.1152/ajpregu.2001.280.3.R790.
7. **Viscarra JA**, **Rodriguez R**, **Vazquez-Medina JP**, **Lee A**, **Tift MS**, **Tavoni SK**, **Crocker DE**, **Ortiz RM.** Insulin and GLP-1 infusions demonstrate the onset of adipose-specific insulin resistance in a large fasting mammal: potential glucogenic role for GLP-1. *Physiol Rep* 1: e00023, 2013.
8. **Castellini MA**, **Costa DP.** Relationships between plasma ketones and fasting duration in neonatal elephant seals. *Am J Physiol* 259: R1086–R1089, 1990.
9. **Cherel Y**, **Robin JP**, **Heitz A**, **Calgari C**, **Le Maho Y.** Relationships between lipid availability and protein utilization during prolonged fasting. *J Comp Physiol B* 162: 305–313, 1992. doi:10.1007/BF00260757.
10. **Orskov C.** Glucagon-like peptide-1, a new hormone of the entero-insular axis. *Diabetologia* 35: 701–711, 1992.
11. **Viscarra JA**, **Vázquez-Medina JP**, **Crocker DE**, **Ortiz RM.** Glut4 is upregulated despite decreased insulin signaling during prolonged fasting in northern elephant seal pups. *Am J Physiol Regul Integr Comp Physiol* 300: R150–R154, 2011. doi:10.1152/ajpregu.00478.2010.
12. **Viscarra JA**, **Vázquez-Medina JP**, **Rodriguez R**, **Champagne CD**, **Adams SH**, **Crocker DE**, **Ortiz RM.** Decreased expression of adipose CD36 and FATP1 are associated with increased plasma nonesterified fatty acids during prolonged fasting in northern elephant seal pups (*Mirounga angustirostris*). *J Exp Biol* 215: 2455–2464, 2012. doi:10.1242/jeb.069070.
13. **Houser DS**, **Champagne CD**, **Crocker DE.** A non-traditional model of the metabolic syndrome: the adaptive significance of insulin resistance in fasting-adapted seals. *Front Endocrinol* 4: 164, 2013. doi:10.3389/fendo.2013.00164.
14. **Viscarra JA**, **Champagne CD**, **Crocker DE**, **Ortiz RM.** 5′AMP-activated protein kinase activity is increased in adipose tissue of northern elephant seal pups during prolonged fasting-induced insulin resistance. *J Endocrinol* 209: 317–325, 2011. doi:10.1530/JOE-11-0017.
15. **Ashmore J.** The effects of glucocorticoids on insulin action: hormonal modifiers of insulin action, New York Diabetes Association Symposium, Part II, October 12, 1963. *Diabetes* 13: 349–354, 1964. doi:10.2337/diab.13.4.349.
16. **Clerc D**, **Wick H**, **Keller U.** Acute cortisol excess results in unimpaired insulin action on lipolysis and branched chain amino acids, but not on glucose kinetics and C-peptide concentrations in man. *Metabolism* 35: 404–410, 1986. doi:10.1016/0026-0495(86)90128-9.
17. **Olmstead KI**, **La Frano MR**, **Fahrmann J**, **Grapov D**, **Viscarra JA**, **Newman JW**, **Fiehn O**, **Crocker DE**, **Filipp FV**, **Ortiz RM.** Insulin induces a shift in lipid and primary carbon metabolites in a model of fasting-induced insulin resistance. *Metabolomics* 13: 60, 2017. doi:10.1007/s11306-017-1186-y.
18. **Johnson KMS**, **Edgerton DS**, **Rodewald T**, **Scott M**, **Farmer B**, **Neal D**, **Cherrington AD.** Intraportal GLP-1 infusion increases nonhepatic glucose utilization without changing pancreatic hormone levels. *Am J Physiol Endocrinol Metab* 293: E1085–E1091, 2007. doi:10.1152/ajpendo.00275.2007.
19. **Seghieri M**, **Rebelos E**, **Gastaldelli A**, **Astiarraga BD**, **Casolaro A**, **Barsotti E**, **Pocai A**, **Nauck M**, **Muscelli E**, **Ferrannini E.** Direct effect of GLP-1 infusion on endogenous glucose production in humans. *Diabetologia* 56: 156–161, 2013. doi:10.1007/s00125-012-2738-3.
20. **Fowler MA**, **Champagne CD**, **Houser DS**, **Crocker DE.** Hormonal regulation of glucose clearance in lactating northern elephant seals (*Mirounga angustirostris*). *J Exp Biol* 211: 2943–2949, 2008. doi:10.1242/jeb.018176.
21. **Fiehn O**, **Wohlgemuth G**, **Scholz M**, **Kind T**, **Lee DY**, **Lu Y**, **Moon S**, **Nikolau B.** Quality control for plant metabolomics: reporting MSI-compliant studies. *Plant J Cell J* 53: 691–704, 2008. doi:10.1111/j.1365-313X.2007.03387.x.
22. **Fiehn O**, **Wohlgemuth G**, **Scholz M.** Setup and annotation of metabolomic experiments by integrating biological and mass spectrometric metadata. In: *Data Integration in the Life Sciences*, edited by Ludäscher B, Raschid L. Berlin, Heidelberg: Springer, 2005, p**.** 224–239.
23. **Scholz M**, **Fiehn O.** SetupX—A Public Study Design Database For Metabolomic Projects. *Biocomputing* 2007. December 2006, p. 169–180.
24. **Barupal DK**, **Haldiya PK**, **Wohlgemuth G**, **Kind T**, **Kothari SL**, **Pinkerton KE**, **Fiehn O.** MetaMapp: mapping and visualizing metabolomic data by integrating information from biochemical pathways and chemical and mass spectral similarity. *BMC Bioinformatics* 13: 99, 2012. doi:10.1186/1471-2105-13-99.
25. **Cao Y**, **Jiang T**, **Girke T.** A maximum common substructure-based algorithm for searching and predicting drug-like compounds. *Bioinformatics* 24: i366–i374, 2008. doi:10.1093/bioinformatics/btn186.
26. **Shannon P**, **Markiel A**, **Ozier O**, **Baliga NS**, **Wang JT**, **Ramage D**, **Amin N**, **Schwikowski B**, **Ideker T.** Cytoscape: a software environment for integrated models of biomolecular interaction networks. *Genome Res* 13: 2498–2504, 2003. doi:10.1101/gr.1239303.
27. **Su G**, **Kuchinsky A**, **Morris JH**, **States DJ**, **Meng F.** GLay: community structure analysis of biological networks. *Bioinformatics* 26: 3135–3137, 2010. doi:10.1093/bioinformatics/btq596.
28. **Barupal DK**, **Fiehn O.** Chemical similarity enrichment analysis (ChemRICH) as alternative to biochemical pathway mapping for metabolomic datasets. *Sci Rep* 7: 1–11, 2017.]doi:10.1038/s41598-016-0028-x.
29. **Houser DS**, **Costa DP.** Protein catabolism in suckling and fasting northern elephant seal pups (*Mirounga anglstirostris*). *J Comp Physiol B* 171: 635–642, 2001. doi:10.1007/s003600100214.
30. **Houser DS**, **Crocker DE**, **Tift MS**, **Champagne CD.** Glucose oxidation and nonoxidative glucose disposal during prolonged fasts of the northern elephant seal pup (*Mirounga angustirostris*). *Am J Physiol Regul Integr Comp Physiol* 303: R562–R570, 2012. doi:10.1152/ajpregu.00101.2012.
31. **Ortiz RM**, **Noren DP**, **Ortiz CL**, **Talamantes F.** GH and ghrelin increase with fasting in a naturally adapted species, the northern elephant seal (*Mirounga angustirostris*). *J Endocrinol* 178: 533–539, 2003. doi:10.1677/joe.0.1780533.
32. **Munro IC**, **Berndt WO**, **Borzelleca JF**, **Flamm G**, **Lynch BS**, **Kennepohl E**, **Bär EA**, **Modderman J**, **Bernt WO.** Erythritol: an interpretive summary of biochemical, metabolic, toxicological and clinical data. *Food Chem Toxicol Int J Publ Br Ind Biol Res Assoc* 36: 1139–1174, 1998. doi:10.1016/S0278-6915(98)00091-X.
33. **Champagne CD**, **Houser DS**, **Fowler MA**, **Costa DP**, **Crocker DE.** Gluconeogenesis is associated with high rates of tricarboxylic acid and pyruvate cycling in fasting northern elephant seals. *Am J Physiol Regul Integr Comp Physiol* 303: R340–R352, 2012. doi:10.1152/ajpregu.00042.2012.

Downloaded from journals.physiology.org/journal/ajpregu by Rudy Ortiz (098.239.103.052) on April 7, 2021.